Relativistic multireference many-body perturbation theory for quasidegenerate systems: Energy levels of ions of the oxygen isoelectronic sequence

Marius J. Vilkas and Yasuyuki Ishikawa
Department of Chemistry, University of Puerto Rico, P.O. Box 23346, San Juan, Puerto Rico 00931-3346

Konrad Koc
Department of Physics, Pedagogical University, Podchorazych 2, 30-084 Krakow, Poland
(Received 16 April 1999; revised manuscript received 15 June 1999)

A relativistic multireference many-body perturbation theory for quasidegenerate systems with multiple open valence shells is developed and implemented with analytic basis sets of Gaussian spinors. The theory employs a general class of multiconfigurational Dirac-Fock self-consistent-field wave functions as reference functions, and thus is applicable to open-shell systems with near degeneracy of a manifold of strongly interacting configurations. A procedure is described by which to perform multireference second-order Møller-Plesset perturbation calculations for a general class of reference functions constructed from one-particle Dirac spinors. Multireference perturbation calculations are reported for the ground and low-lying excited states of oxygen and oxygenlike ions with up to a nuclear charge of $Z=60$ in which the near degeneracy of a manifold of strongly interacting configurations mandates a multireference treatment. [S1050-2947(99)03110-8]

PACS number(s): 31.25.−v, 31.30.Jv, 31.25.Jf

I. INTRODUCTION

Over the years most relativistic atomic structure calculations have been carried out by either a finite-difference multiconfiguration (MC) Dirac-Fock self-consistent-field (DF SCF) [1–4] or a relativistic many-body perturbation theory (MBPT) based on single-configuration DF SCF wave functions expanded in analytic basis sets [5–10]. Each of these methods has strengths and weaknesses because their accuracy is restricted to different sectors of a many-electron correlation. The MCDFSCF method is most effective in treating nondynamic correlation (i.e., near degeneracy in the valence shells), but fails to account for the bulk of dynamic correlation. The single-reference many-body perturbation theory has exactly the opposite characteristic; it is effective in accurately describing dynamic correlation but fails to account for nondynamic correlation. Dynamic correlation is a short-range effect that arises from electron-electron interaction and is the major correction to the Dirac-Fock independent particle model, while nondynamic correlation is a consequence of the existence of nearly degenerate excited states that interact strongly with the reference state [11–16]. Systems in which only the dynamic correlation is important may be described by a single configuration DF wave function, whereas systems with significant nondynamic correlation cannot be correctly described within single-configuration DF wave functions.

Near degeneracy in the valence spinors gives rise to a manifold of strongly interacting configurations, i.e., strong configuration mixing within a relativistic complex [11], and makes a MC treatment mandatory. The classic examples in atomic physics are the near-degeneracy effects in ground-state beryllium [11,12,17] and openshell atoms with two or more open valence shells [11,13–16]. For reactive and excited-state energy surfaces of molecules, the single configuration SCF theory also fails to properly describe the separated fragments because of the near degeneracy that follows the separation process [18–20]. As Weiss and Kim showed [11], relativity alters the magnitude of configuration mixing among the configuration-state functions (CSFs) as Z increases in an isoelectronic sequence. For low-Z ions energy levels are clustered together according to their n quantum number occupancy (i.e., nonrelativistic complex [21]), but as Z increases, they cluster together according to both their n and j quantum number occupancy (i.e., relativistic complex [11]). Strong configuration interaction within a complex due to asymptotic degeneracy is called asymptotic configuration interaction (CI). By including in a zero-order multiconfiguration reference function all the CSFs generated within a complex of given principal quantum number n, relativistic multireference perturbation theory is capable of recovering dynamic correlation energy throughout the isoelectronic sequence. Alteration in the clustering pattern, i.e., asymptotic CI, in increasing Z may be easily accounted for in zero order by relativistic MCDFSCF. Thus MCDFSCF based on all the CSFs generated within a nonrelativistic complex, is capable of accounting for nondynamic correlation from low to high Z even when the configuration interaction is altered as Z increases.

Once the near-degeneracy effects in a complex [11] are accounted for by matrix MCDFSCF [22], the remaining dynamic correlation may be recovered either by a relativistic generalization of a nonrelativistic multireference Møller-Plesset (MRMP) perturbation theory [18], or by a multireference configuration interaction based on the MCDFSCF reference functions [16,22]. The multireference configuration-interaction approach [16,22], however, becomes quickly unwieldy in systems with large numbers of electrons because the order of the multireference configuration-interaction matrix increases rapidly as the number of electrons increases [15,18]. Hirao [18] argues that once the state-specific nondynamic correlation among valence electrons is treated by multiconfiguration Hartree-Fock wave functions, the remaining

correlation may be recovered by second-order perturbation theory because it consists mainly of dynamic pair correlation due to short-range fluctuation potentials. In the present study, we develop a relativistic MRMP theory that combines the strengths of both MCDFSCF and many-body perturbation methods in application to a general class of quasidegenerate systems with multiple open valence shells. We extend the single-reference relativistic many-body perturbation theory [5–8] to a relativistic MR-MP perturbation theory for systems with a manifold of strongly interacting configurations. The essential feature of the theory is its treatment of the state-specific nondynamic correlation in zero order through quadratically convergent matrix MCDFSCF [22], and recovery of the remaining correlation, which is predominantly dynamic pair correlation, by second-order MR-MP perturbation theory.

We report here the successful implementation and application of a relativistic MRMP perturbation theory, which takes a general class of MCDFSCF wave functions as reference functions. The multiconfiguration wave functions are computed by a recently developed quadratically convergent matrix MCDFSCF method [22] in analytic basis sets of G spinors (G for Gaussian after Grant [23]). A procedure is described by which to perform a relativistic second-order MR-MP perturbation theory calculations for a general class of MC reference functions constructed from Dirac natural spinors. The state-specific multireference perturbation calculations are reported for the ground and low-lying excited states of ions of the oxygen isoelectronic sequence in which the near degeneracy of a manifold of strongly interacting configurations necessitates a relativistic multireference perturbation treatment.

II. THEORY

A. The relativistic no-pair Dirac-Coulomb-Breit Hamiltonian

The effective N-electron Hamiltonian (in atomic units) for the development of our MRMP algorithm is taken to be the relativistic ''no-pair'' Dirac-Coulomb (DC) Hamiltonian [24,25],

$$H_{\mathrm{DC}}^{+}=\sum_{i}^{N} h_D(i)+\mathcal{L}_{+}\left(\sum_{i>j}^{N}\frac{1}{r_{ij}}\right)\mathcal{L}_{+}. \tag{1}$$

$\mathcal{L}_{+}=L_{+}(1)L_{+}(2),\ldots,L_{+}(N)$, where $L_{+}(i)$ is the projection operator onto the space $D^{(+)}$ spanned by the positive-energy eigenfunctions of the matrix DFSCF equation [25]. $\mathcal{L}_{+}$ is the projection operator onto the positive-energy space $\mathfrak{D}^{(+)}$ spanned by the N-electron CSFs constructed from the positive-energy eigenfunctions ($\in D^{(+)}$) of the matrix DF SCF. It takes into account the field-theoretic condition that the negative-energy states are filled and causes the projected DC Hamiltonian to have normalizable bound-state solutions. This approach is called the no-pair approximation [24] because virtual electron-positron pairs are not permitted in the intermediate states. The eigenfunctions of the matrix DF SCF equation clearly separate into two discrete manifolds, $D^{(+)}$ and $D^{(-)}$, respectively, of positive-energy and negative-energy states. As a result, the positive-energy projection operators can be accommodated easily in many-body calculations. The formal conditions on the projection are automatically satisfied when only the positive-energy spinors ($\in D^{(+)}$) are employed. h_D is the Dirac one-electron Hamiltonian (in a.u.),

$$h_D(i)=c(\alpha_i\cdot\mathbf{p}_i)+(\beta_i-1)c^2+V_{\mathrm{nuc}}(r_i). \tag{2}$$

Here α and β are the 4×4 Dirac vector and scalar matrices, respectively. $V_{\mathrm{nuc}}(r)$ is the nuclear potential, which for each nucleus takes the form

$$V_{\mathrm{nuc}}(r)=\begin{cases}-\dfrac{Z}{r}, & r>R\\[2ex] -\dfrac{Z}{2R}\left(3-\dfrac{r^2}{R^2}\right), & r\leqslant R.\end{cases} \tag{3}$$

The nuclei are modeled as spheres of a uniform proton-charge distribution; Z is the nuclear charge, R (Bohr) is the radius of that nucleus and is related to the atomic mass, A (amu), by $R=2.2677\times10^{-5}A^{1/3}$. Adding the frequency-independent Breit interaction

$$B_{12}=-\tfrac{1}{2}[\alpha_1\cdot\alpha_2+(\alpha_1\cdot\mathbf{r}_{12})(\alpha_2\cdot\mathbf{r}_{12})/r_{12}^2]/r_{12} \tag{4}$$

to the electron-electron Coulomb interaction in Coulomb gauge results in the Coulomb-Breit potential, which is correct to order α^2 (α being the fine-structure constant) [24]. Addition of the Breit term yields the no-pair Dirac-Coulomb-Breit (DCB) Hamiltonian [24,25]

$$H_{\mathrm{DCB}}^{+}=\sum_{i}^{N} h_D(i)+\mathcal{L}_{+}\left(\sum_{i>j}^{N}\frac{1}{r_{ij}}+B_{ij}\right)\mathcal{L}_{+}, \tag{5}$$

which is covariant to first order and increases the accuracy of calculated fine-structure splittings and inner-electron binding energies. Higher-order QED effects appear first in order α^3.

B. The matrix multiconfiguration Dirac-Fock SCF method

N-electron eigenfunctions of the no-pair DC Hamiltonian are approximated by a linear combination of M configuration-state functions, $\{\Phi_I^{(+)}(\gamma_I\mathcal{J}\pi);\ I=1,2,\ldots,M\}$, constructed from positive-energy eigenfunctions of the matrix DFSCF equation. The M configuration-state functions form a subspace $\mathfrak{B}^{(+)}$ of the positive-energy space $\mathfrak{D}^{(+)}$.

$$\psi_K(\gamma_K\mathcal{J}\pi)=\sum_{I}^{M} C_{IK}\Phi_I^{(+)}(\gamma_I\mathcal{J}\pi). \tag{6}$$

Here the MCDFSCF wave function $\psi_K(\gamma_K\mathcal{J}\pi)$ is an eigenfunction of the angular momentum and parity operators with total angular momentum $\mathcal{J}$ and parity π. γ denotes a set of quantum numbers other than $\mathcal{J}$ and π necessary to specify the state uniquely. The total DC energy of the general MCDF state $|\psi_K(\gamma_K\mathcal{J}\pi)\rangle$ can be expressed as

$$\begin{aligned}E^{MC}(\gamma_K\mathcal{J}\pi)&=\langle\psi_K(\gamma_K\mathcal{J}\pi)|H_{\mathrm{DC}}^{+}|\psi_K(\gamma_K\mathcal{J}\pi)\rangle\\&=\sum_{I,J=1}^{\mathfrak{B}(+)} C_{IK}C_{JK}\\&\quad\times\langle\Phi_I^{(+)}(\gamma_I\mathcal{J}\pi)|H_{\mathrm{DC}}^{+}|\Phi_J^{(+)}(\gamma_J\mathcal{J}\pi)\rangle.\end{aligned} \tag{7}$$

Here it is assumed that $\psi_K(\gamma_K\mathcal{J}\pi)$ and $\Phi_I^{(+)}(\gamma_I\mathcal{J}\pi)$ are normalized.

Given a trial orthonormal set of one-particle radial spinors $\{\phi^{(0)}_{n_q\kappa_q}(r)\}(\in D^{(+)}\cup D^{(-)})$, the optimum occupied electronic radial spinors $\{\phi^{(+)}_{n_p\kappa_p}(r)\}(\in D^{(+)})$ can be found by a unitary transformation $\mathbf{U}=1+\mathbf{T}$ via

$$\begin{aligned}\phi^{(+)}_{n_p\kappa_p}(r)&=\frac{1}{r}\begin{pmatrix}P_{n_p\kappa_p}(r)\\ Q_{n_p\kappa_p}(r)\end{pmatrix}\\&=\sum_{q\in D^{(+)}\cup D^{(-)}}^{2N_\kappa}\phi^{(0)}_{n_q\kappa_q}(r)U_{qp}\\&=\sum_{q}^{2N_\kappa}\phi^{(0)}_{n_q\kappa_q}(r)(T_{qp}+\delta_{qp}).\end{aligned}\tag{8}$$

Here, the summation extends over both N_κ negative and N_κ positive energy spinors. $P_{n_p\kappa_p}(r)$ and $Q_{n_p\kappa_p}(r)$ are the large and small radial components and are expanded in N_κ G spinors, $\{\chi^L_{\kappa i}\}$ and $\{\chi^L_{\kappa i}\}$, that satisfy the boundary conditions associated with the finite nucleus [26],

$$P_{n\kappa}(r)=\sum_i^{N_\kappa}\chi^L_{\kappa i}\xi^L_{ki}\quad\text{and}\quad Q_{n\kappa}(r)=\sum_i^{N_\kappa}\chi^S_{\kappa i}\xi^S_{ki}.\tag{9}$$

Here $\{\xi^L_{ki}\}$ and $\{\xi^S_{ki}\}$ are linear variation coefficients. Second-order variation of the MCDF energy [Eq. (7)] with respect to the parameters $\{T_{qp}\}$ and configuration mixing coefficients $\{C_{IK}\}$ leads to the Newton-Raphson (NR) equations for second-order the MC DFSCF,

$$\begin{pmatrix}g^o_{pe}\\ g^c_\gamma\end{pmatrix}+\sum_{qf\gamma''}\begin{pmatrix}h^{oo}_{pe,gf} & h^{oc}_{pe,\gamma''}\\ h^{co}_{\gamma',gf} & h^{cc}_{\gamma',\gamma''}\end{pmatrix}\begin{pmatrix}T_{qf}\\ B_{\gamma''}\end{pmatrix}=\begin{pmatrix}0\\0\end{pmatrix}.\tag{10}$$

Here g^o_{pe}, g^c_γ, $h^{oo}_{pe,gf}$, etc. are those defined in previous work [22]. Intermediate coupling is built in through the MCDF SCF process. The quadratically convergent NR algorithm for relativistic MCDFSCF calculations has been discussed in detail in previous work [22] and is not discussed further. To remove the arbitrariness of the MC SCF spinors and density weighting, the canonical SCF spinors are transformed into natural spinors $\{\omega^{(+)}_{n_p\kappa_p}\}$ for subsequent perturbation calculations [18]. The key to successful implementation of the subsequent MRMP perturbation theory calculations is rapid convergence of our quadratically convergent matrix MCDFSCF method [22] for a general class of MCDF wave functions for openshell quasidegenerate systems.

C. Relativistic multireference many-body perturbation theory

The no-pair DC Hamiltonian $H^+_{\rm DC}$ is partitioned into an unperturbed Hamiltonian and a perturbation term following Møller and Plesset [27],

$$H^+_{\rm DC}=H_0+V,\tag{11}$$

where the unperturbed model Hamiltonian H_0 is a sum of ''average'' DF operators $F_{\rm av}$,

$$H_0=\sum_i^N F_{av}(i)\quad\text{and}\quad V=H^+_{\rm DC}-\sum_i^N F_{av}(i).\tag{12}$$

Here, the one-body operator F_{av} diagonal in $\{\omega^{(+)}_{n_p\kappa_p}\}$ may be defined by

$$\begin{aligned}F_{\rm av}&=\sum_{p\in D(+)}|\omega^{(+)}_{n_p\kappa_p}\rangle\langle\omega^{(+)}_{n_p\kappa_p}|f_{av}|\omega^{(+)}_{n_p\kappa_p}\rangle\langle\omega^{(+)}_{n_p\kappa_p}|\\&=\sum_{p\in D(+)}|\omega^{(+)}_{n_p\kappa_p}\rangle\varepsilon^+_p\langle\omega^{(+)}_{n_p\kappa_p}|,\end{aligned}\tag{13}$$

where

$$\varepsilon^+_p=\langle\omega^{(+)}_{n_p\kappa_p}|f_{av}|\omega^{(+)}_{n_p\kappa_p}\rangle\quad\text{and}\quad f_{av}=h_D+\sum_p^{occ}\tilde{n}_p(J_p-K_p).\tag{14}$$

The generalized fractional occupation $\tilde{n}_p$ is related to diagonal matrix elements of the first-order reduced density matrix constructed in natural spinors by

$$\tilde{n}_p=D_{pp}=\sum_I^{\mathfrak{B}(+)}C_{IK}C_{IK}n_{n_p\kappa_p}[I],\tag{15}$$

where $n_{n_p\kappa_p}[I]$ is the occupation number of the κ-symmetry shell in the CSF $\Phi_I(\gamma_I\mathcal{J}\pi)$. J_p and K_p are the usual Coulomb and exchange operators constructed in natural spinors.

The unperturbed Hamiltonian H_0 may be given in second quantized form,

$$H_0=\sum_{p\in D(+)}\{a^\dagger_pa_p\}\varepsilon^+_p,\tag{16}$$

where $\{a^\dagger_pa_p\}$ is a normal product of creation and annihilation operators, $a^\dagger_p$ and a_p, respectively. The zero-order Hamiltonian H_0 is arbitrary but should be chosen as close to the full Hamiltonian $H^+_{\rm DC}$ as possible so that the perturbation series converges rapidly in low order. The zero-order Hamiltonian is usually chosen to be a sum of effective one-electron operators (Møller-Plesset partitioning [27]). For closed-shell systems, the best results have been obtained with Møller-Plesset partitioning, i.e., the sum of closed-shell Fock operators as H_0. An effective one-body operator for a general MC DFSCF closely related to the closed-shell Fock operator is the ''average'' DF operator F_{av}, a relativistic generalization of a nonrelativistic average Fock operator [18]. The theory provides a hierarchy of well-defined algorithms that allows one to calculate relativistic correlation corrections in noniterative steps and, in low order, yields a large fraction of the dynamical correlation. In this form of partitioning, perturbation corrections describe relativistic electron correlation, including cross contributions between relativistic and correlation effects.

Many-electron wave functions correct to α^2 may be expanded in a set of CSFs that spans the entire N-electron positive-energy space $\mathfrak{D}^{(+)}$, $\{\Phi^{(+)}_I(\gamma_I\mathcal{J}\pi)\}$, constructed in terms of Dirac one-electron spinors. Individual CSFs are eigenfunctions of the total angular momentum and parity operators and are linear combinations of antisymmetrized prod-

ucts of positive-energy spinors ($\in D^{(+)}$). The one-electron spinors are mutually orthogonal so the CSFs $\{\Phi_I^{(+)}(\gamma_I\mathcal{J}\pi)\}$ are mutually orthogonal. The unperturbed Hamiltonian is diagonal in this space;

$$H_0=\sum_I^{\mathfrak{D}(+)} |\Phi_I^{(+)}(\gamma_I\mathcal{J}\pi)\rangle E_I^{\mathrm{CSF}}\langle\Phi_I^{(+)}(\gamma_I\mathcal{J}\pi)|, \quad (17)$$

so that

$$H_0|\Phi_I^{(+)}(\gamma_I\mathcal{J}\pi)\rangle=E_I^{\mathrm{CSF}}|\Phi_I^{(+)}(\gamma_I\mathcal{J}\pi)\rangle \quad (I=1,2,\ldots). \quad (18)$$

Since the zero-order Hamiltonian is defined as a sum of one-electron operators F_{av} [Eq. (12)], E_I^{CSF} is a sum of the products of one-electron energies defined by ε_q^+ and an occupation number $n_{n_q\kappa_q}[I]$ of the κ_q-symmetry shell in the CSF $\Phi_I^{(+)}(\gamma_I\mathcal{J}\pi)$;

$$E_I^{\mathrm{CSF}}=\sum_q^{D(+)} \varepsilon_q^+ n_{n_q\kappa_q}[I]. \quad (19)$$

The subset, $\{\Phi_I^{(+)}(\gamma_I\mathcal{J}\pi);I=1,2,\ldots,M\}$, with which we expand the MCDFSCF function $\psi_K(\gamma_K\mathcal{J}\pi)$ [Eq. (6)] also defines an active subspace $\mathfrak{B}^{(+)}$ spanned by $\psi_K(\gamma_K\mathcal{J}\pi)$ and its $M-1$ orthogonal complements, $\{\psi_K(\gamma_K\mathcal{J}\pi);K=1,2,\ldots,M\}$. The matrix of H_{DC}^+ in this subspace is diagonal

$$\begin{aligned}\langle\psi_K(\gamma_K\mathcal{J}\pi)|H_{\mathrm{DC}}^+|\psi_L(\gamma_L\mathcal{J}\pi)\rangle&=\delta_{KL}(E_K^{(0)}+E_K^{(1)})\\&=\delta_{KL}E^{MC}(\gamma_K\mathcal{J}\pi),\end{aligned} \quad (20)$$

where

$$\begin{aligned}E_K^{(0)}&=\langle\psi_K(\gamma_K\mathcal{J}\pi)|H_0|\psi_K(\gamma_K\mathcal{J}\pi)\rangle\\&=\sum_I^M C_{IK}C_{IK}E_I^{\mathrm{CSF}}=\sum_p^{occ}\varepsilon_p^+\tilde{n}_p\end{aligned}$$

and

$$E_K^{(1)}=\langle\psi_K(\gamma_K\mathcal{J}\pi)|V|\psi_K(\gamma_K\mathcal{J}\pi)\rangle.$$

The residual space in the positive-energy subspace is $\mathfrak{Q}^{(+)}=\mathfrak{D}^{(+)}-\mathfrak{B}^{(+)}$, which is spanned by CSFs $\{\Phi_I^{(+)}(\gamma_I\mathcal{J}\pi);\ I=M+1,M+2,\ldots\}$.

Application of Rayleigh-Schrödinger perturbation theory provides order-by-order expressions of the perturbation series for the state approximated by $|\psi_K(\gamma_K\mathcal{J}\pi)\rangle$,

$$E_K(\gamma_K\mathcal{J}\pi)=E^{MC}(\gamma_K\mathcal{J}\pi)+E_K^{(2)}+E_K^{(3)}+\cdots, \quad (21)$$

where

$$E_K^{(2)}=\langle\psi_K(\gamma_K\mathcal{J}\pi)|V\mathcal{R}V|\psi_K(\gamma_K\mathcal{J}\pi)\rangle \quad (22)$$

and

$$E_K^{(3)}=\langle\psi_K(\gamma_K\mathcal{J}\pi)|V\mathcal{R}(H_0-E_K^{(1)})\mathcal{R}V|\psi_K(\gamma_K\mathcal{J}\pi)\rangle. \quad (23)$$

Here, $\mathcal{R}$ is the resolvent operator,

$$\mathcal{R}=\frac{\mathcal{Q}^{(+)}}{E_K^{(0)}-H_0}$$

with

$$\mathcal{Q}^{(+)}=\sum_I^{\mathfrak{Q}(+)} |\Phi_I^{(+)}(\gamma_I\mathcal{J}\pi)\rangle\langle\Phi_I^{(+)}(\gamma_I\mathcal{J}\pi)|. \quad (24)$$

The projection operator $\mathcal{Q}^{(+)}$ projects onto the subspace $\mathfrak{Q}^{(+)}$ spanned by CSFs $\{\Phi_I^{(+)}(\gamma_I\mathcal{J}\pi);\ I=M+1,M+2,\ldots\}$. Using the spectral resolution of the resolvent operator acting on $V|\Phi_I^{(+)}(\gamma_I\mathcal{J}\pi)\rangle$, the second-order correction may be expressed as

$$\begin{aligned}E_K^{(2)}&=\sum_{IJ} C_{IK}C_{JK}\langle\Phi_I^{(+)}(\gamma_I\mathcal{J}\pi)|V\mathcal{R}V|\Phi_J^{(+)}(\gamma_J\mathcal{J}\pi)\rangle\\&=\sum_{L=M+1}^{\mathfrak{Q}(+)}\sum_{I,J=1}^{\mathfrak{B}(+)} C_{IK}C_{JK}\frac{\langle\Phi_I^{(+)}(\gamma_I\mathcal{J}\pi)|V|\Phi_L^{(+)}(\gamma_L\mathcal{J}\pi)\rangle\langle\Phi_L^{(+)}(\gamma_L\mathcal{J}\pi)|V|\Phi_J^{(+)}(\gamma_J\mathcal{J}\pi)\rangle}{E_J^{\mathrm{CSF}}-E_L^{\mathrm{CSF}}}.\end{aligned} \quad (25)$$

In this form, all perturbation corrections beyond first-order describe relativistic electron correlation for the state approximated by the MCDFSCF wave function $|\psi_K(\gamma_K\mathcal{J}\pi)\rangle$. When the effective electron-electron interaction is approximated by the instantaneous Coulomb interaction $1/r_{ij}$, relativistic electron correlation is termed a DC correlation [8]. Inclusion of the frequency-independent Breit interaction in the effective electron-electron interaction yields the no-pair DCB Hamiltonian [Eq. (5)], and the relativistic electron correlation arising from the DCB Hamiltonian is the DCB correlation [8].

Summations over the CSFs in Eqs. (17)–(25) are restricted to CSFs ($\in\mathfrak{D}^{(+)}$) constructed from the positive-energy branch ($D^{(+)}$) of the spinors, effectively incorporating into the computational scheme the ''no-pair'' projection operator $\mathcal{L}_+$ contained in the DC and DCB Hamiltonians.

Further, the CSFs $\Phi_L^{(+)}(\gamma_L \mathcal{J}\pi)(\in \mathfrak{Q}^{(+)})$ generated by excitations higher than double, relative to the reference CSFs $\Phi_I^{(+)}(\gamma_I \mathcal{J}\pi)(\in \mathfrak{B}^{(+)})$, do not contribute to the second- and third-order because for them

$$\langle \Phi_I^{(+)}(\gamma_I \mathcal{J}\pi)|V|\Phi_L^{(+)}(\gamma_L \mathcal{J}\pi)\rangle = 0$$

and

$$\langle \Phi_I^{(+)}(\gamma_I \mathcal{J}\pi)|H_{\mathrm{DC}}^{+}|\Phi_L^{(+)}(\gamma_L \mathcal{J}\pi)\rangle = 0.$$

Neglecting interactions with the filled negative-energy sea, i.e., neglecting virtual electron-positron pairs in summing the MBPT diagrams, we have a straightforward extension of nonrelativistic MBPT. Negative-energy states $(\in D^{(+)})$, as part of the complete set of states, do play a role in higher-order QED corrections. Studies have appeared, which go beyond the ''no-pair'' approximation where negative-energy states are needed to evaluate the higher-order QED effects [28–33]. Contributions from the negative-energy states due to creation of virtual electron-positron pairs are of the order α^3 [28–33], and estimations of the radiative corrections are necessary in order to achieve spectroscopic accuracy for higher Z. In the present study, the lowest-order radiative corrections were estimated for each state to achieve better accuracy.

III. COMPUTATION

The large radial component is expanded in a set of Gaussian-type functions (GTFs) [26],

$$\chi_{\kappa i}^{L}(r) = A_{\kappa i}^{L} r^{n[\kappa]} \exp(-\zeta_{\kappa i} r^2), \tag{26}$$

with $n[\kappa] = -\kappa$ for $\kappa < 0$ and $n[\kappa] = \kappa + 1$ for $\kappa > 0$. $A_{\kappa i}^{L}$ is the normalization constant. The small component basis set $\{\chi_{\kappa i}^{S}(r)\}$ is constructed to satisfy the boundary condition associated with the finite nucleus with a uniform proton charge distribution [26]. With the finite nucleus, GTFs of integer power of r are especially appropriate basis functions because the finite nuclear boundary results in a solution that is Gaussian at the origin [26]. Basis functions, which satisfy the nuclear boundary conditions, are also automatically kinetically balanced. Imposition of the boundary conditions results in particularly simple forms with spherical G spinors [26].

For all the oxygenlike systems studied, even-tempered basis sets [34] of $26s22p$ Gaussian-type were used for the MCDFSCF. In basis sets of even-tempered Gaussians, the exponents, $\{\zeta_{\kappa i}\}$ are given in terms of the parameters, α and β, according to the geometric series

$$\zeta_{\kappa i} = \alpha \beta^{i-1}, \quad i = 1,2,\ldots,N_{\kappa} \tag{27}$$

In MCDFSCF calculations on oxygenlike species, the parameters α and β are optimized until a minimum in the DF total energy is found. The optimal α and β values thus determined for, e.g., oxygenlike neon $(Z=10)$ are, respectively, 0.148055 and 2.11. The radial functions that possess a different κ quantum number but the same quantum number ℓ are expanded in the same set of basis functions (e.g., the radial functions of $p_{1/2}$ and $p_{3/2}$ symmetries are expanded in the same set of p-type radial Gaussian-type functions). The nuclei were again modeled as spheres of uniform proton charge in every calculation. The nuclear model has been discussed in detail in Ref. [26].

Virtual spinors used in the MRMP perturbation calculations were generated in the field of the nucleus and all electrons (V^N potential) by employing the ''average'' DF operator F_{av} [Eq. (13)]. The order of the partial-wave expansion, $L_{\max}$, the highest angular momentum of the spinors included in the virtual space, is $L_{\max}=7$ (a $26s22p20d18f16g16h16i16j$ G spinor basis set) throughout this study. All-electron MRMP perturbation calculations including the frequency-independent Breit interaction in the first and second orders of perturbation theory are based on the no-pair Dirac-Coulomb-Breit Hamiltonian, H_{DCB}^{+}. The speed of light was taken to be 137.035 989 5 a.u. Radiative corrections, or the Lamb shifts, were estimated for each state by evaluating the electron self-energy and vacuum polarization following an approximation scheme discussed by Indelicato, Gorceix, and Desclaux [33]. The code described in Refs. [33] and [35] was adapted to our basis-set expansion calculations for this purpose. In this scheme [35], the screening of the self-energy is estimated by employing the charge density of a spinor integrated to a short distance from the origin, typically an 0.3 Compton wavelength. The ratio of the integral computed with an MCDFSCF spinor and that obtained by using the corresponding hydrogenic spinor is used to scale the self-energy correction for a bare nuclear charge computed by Mohr [28]. The effect on the term energy splittings of mass polarization and reduced mass are non-negligible. In the present study, however, we neglect these effects.

IV. RESULTS AND DISCUSSIONS

A substantial number of ground-state atoms are openshell systems with complicated multiplet structures. With six valence electrons, ground and low-lying excited states of oxygenlike ions exhibit the near degeneracy characteristic of a manifold of strongly interacting configurations within the $n=2$ complex [3,11,36]. We first give a detailed account of the MCDFSCF and MRMP calculations applied to oxygenlike ions with $Z=20$ and $Z=30$. Table I displays the computed MCDFSCF energies, E_{SCF}, of the lowest $J=0$ ($^3P_0$), $J=1$ ($^3P_1$), and $J=2$ ($^3P_2$) even-parity states of Ca^{12+} ($Z=20$) and Zn^{22+} ($Z=30$), in increasing number of configurations within the $n=2$ complex. In each entry in the table, we give the number of CSFs, N_{CSF}, that arises from the electronic configurations displayed in the second column. The MCDF energy, E_{SCF}, computed with each of the N_{CSF} CSFs is given in the third column. In the MCDFSCF calculations, the $1s$ spinor was kept doubly occupied and the remaining six electrons were treated as active electrons in generating CSFs within the $n=2$ shells. MCDFSCF calculations on Ca^{12+} were performed to obtain a single set of spinors for all the $^3P_{J=0,1,2}$ fine-structure states by optimizing the J-averaged MC energies: $E_{J\text{-}ave}^{\mathrm{MC}}(\gamma_K\pi) = \Sigma_{J=0,1,2}(2J+1)E^{\mathrm{MC}}(\gamma_K J\pi)/\Sigma_{J'}(2J'+1)$ instead of performing state-specific MCDFSCF calculations on each fine-structure state. For low-Z ions with small fine-structure splittings (i.e., near degeneracy among $2p_{1/2}$ and $2p_{3/2}$ spinors), the approach is more effective in computing the fine-structure splittings. For

TABLE I. MCDFSCF and second-order MRMP energies (a.u.) of the lowest $J=2$ ($^3P_2$), $J=0$ ($^3P_0$), and $J=1$ ($^3P_1$) even-parity states of Ca^{12+} ($Z=20$) and Zn^{22+} ($Z=30$) computed in increasing CSF-expansion length. Notations $2p_- = 2p_{1/2}$ and $2p_+ = 2p_{3/2}$ were used.

N_{CSF}	CSF	E_{SCF}[a]	E_{corr}^{MC}[b]	$E_{DC}^{(2)}$[c]	$E_{corr}^{MC}+E_{DC}^{(2)}$
		Ca^{12+}			
		$^3P_2$			
1	$2s^2 2p_-^2 2p_+^2$	−597.364 573	0.0	−0.302 030	−0.302 030
2	$2s^2 2p_-^2 2p_+^2, 2s^2 2p_- 2p_+^3$	−597.440 366	−0.075 793	−0.282 744	−0.358 537
		$^3P_0$			
1	$2s^2 2p_-^2 2p_+^2$	−596.911 937	0.0	−0.396 032	−0.396 032
2	$2s^2 2p_-^2 2p_+^2, 2s^2 2p_+^4$	−597.303 633	−0.391 696	−0.285 847	−0.677 543
3	$2s^2 2p_-^2 2p_+^2, 2s^2 2p_+^4, 2p_-^2 2p_+^4$	−597.308 649	−0.396 712	−0.282 744	−0.679 456
		$^3P_1$			
1	$2s^2 2p_- 2p_+^3$	−597.328 018	0.0	−0.283 400	−0.283 400
		Zn^{22+}			
		$^3P_2$			
1	$2s^2 2p_-^2 2p_+^2$	−1428.718 893	0.0	−0.315 314	−0.315 314
2	$2s^2 2p_-^2 2p_+^2, 2s^2 2p_- 2p_+^3$	−1428.775 842	−0.056 949	−0.297 610	−0.354 559
		$^3P_0$			
1	$2s^2 2p_-^2 2p_{3/2}^2$	−1427.982 733	0.0	−0.442 840	−0.442 840
2	$2s^2 2p_-^2 2p_+^2, 2s^2 2p_+^4$	−1428.232 123	−0.249 390	−0.324 875	−0.574 265
3	$2s^2 2p_-^2 2p_+^2, 2s^2 2p_+^4, 2p_-^2 2p_+^4$	−1428.290 915	−0.308 182	−0.288 872	−0.597 054
		$^3P_1$			
1	$2s^2 2p_- 2p_+^3$	−1427.952 955	0.0	−0.295 526	−0.295 526

[a]MCDFSCF energy.

[b]Correlation energy recovered from the MCDFSCF by substracting the single configuration DFSCF energy from the MCDFSCF energies.

[c]Second-order DC correlation correction obtained by MR-MP.

Zn^{22+}, an optimized set of spinors was obtained for each of the $J=0,1,2$ fine-structure states by state-specific MCDF SCF calculations.

The configuration mixing coefficients for the ground and low-lying excited $J=0$, 1, and 2 even-parity states of a Ca^{12+} and Zn^{22+} are reproduced in Table II for comparison. The magnitude of the configuration mixing coefficients is a measure of configuration interaction. The electronic configurations, $2s^2 2p_{1/2}^2 2p_{3/2}^2$, $2s^2 2p_{3/2}^4$, and $2p_{1/2}^2 2p_{3/2}^4$, give rise to three $J=0$ even-parity states (one $^3P_0$ state and two $^1S_0$ states), and they do interact strongly. As we stated earlier, $2p_{1/2}$ and $2p_{3/2}$ spinors are nearly degenerate in a low-Z Ca^{12+} ion because relativistic effects are very small (i.e., weak spin-orbit coupling), and consequently the CSFs aris-

TABLE II. Configuration-mixing coefficients for the ground and low-lying excited $J=0$, $J=1$, and $J=2$ even-parity states of Ca^{12+} and Zn^{22+}.

State	Configuration-mixing coefficient			
$C_{2s^2 2p_{1/2}^2 2p_{3/2}^2}$	$C_{2s^2 2p_{1/2}^1 2p_{3/2}^3}$	$C_{2s^2 2p_{3/2}^4}$	$C_{2p_{1/2}^2 2p_{3/2}^4}$	
		Ca^{12+}		
$^3P_2$	0.903 954	0.427 629	0.0	0.0
$^3P_0$	0.737 246	0.0	−0.674 943	0.030 330
$^3P_1$	0.0	1.000 000	0.0	0.0
$^1D_2$	−0.427 629	0.903 954	0.0	0.0
$^1S_0$	0.663 871	0.0	0.732 027	0.153 008
$^1S_0$	−0.125 474	0.0	−0.092 669	0.987 759
		Zn^{22+}		
$^3P_2$	0.976 913	0.213 639	0.0	0.0
$^3P_0$	0.945 764	0.0	−0.316 661	0.072 506
$^3P_1$	0.0	1.000 000	0.0	0.0
$^1D_2$	−0.213 639	0.976 913	0.0	0.0
$^1S_0$	0.307 382	0.0	0.944 532	0.115 653
$^1S_0$	−0.105 107	0.0	−0.087 093	0.990 640

TABLE III. MC DF SCF energies, E_{SCF}; second-order DC correlation energies, $E_{\mathrm{DC}}^{(2)}$; first- and second-order Breit correlation corrections, $B^{(1)}$ and $B^{(2)}$; and LSs (a.u.) of six even-parity ($2s^2 2p^4$ and $2p^6$) and four odd-parity ($2s2p^5$) states of representative oxygenlike ions.

State	E_{SCF}	$E_{\mathrm{DC}}^{(2)}$	$B^{(1)}$	$B^{(2)}$	LS	E_{total}
			$Z=10$			
$2s^2 2p^4\ {}^3P_2$	−126.519 812	−0.261 388	0.016 270	−0.001 873	0.010 731	−126.756 072
${}^3P_1$	−126.516 848	−0.261 428	0.016 205	−0.001 876	0.010 737	−126.753 210
${}^3p_0$	−126.515 452	−0.261 447	0.016 067	−0.001 882	0.010 740	−126.751 974
${}^1D_2$	−126.392 459	−0.271 229	0.016 161	−0.001 911	0.010 734	−126.638 703
${}^1S_0$	−126.277 142	−0.251 763	0.016 428	−0.001 965	0.010 712	−126.503 729
$2p^6\ {}^1S_0$	−124.126 219	−0.512 837	0.016 416	−0.002 184	0.010 093	−124.614 732
$2s2p^5\ {}^3P_2^o$	−125.542 229	−0.306 242	0.016 257	−0.001 869	0.010 398	−125.823 684
${}^3P_1^o$	−125.539 384	−0.306 129	0.016 037	−0.001 872	0.010 404	−125.820 944
${}^3P_0^o$	−125.537 947	−0.306 189	0.016 029	−0.001 863	0.010 407	−125.819 564
${}^1P_1^o$	−125.089 614	−0.362 225	0.016 223	−0.001 958	0.010 401	−125.427 173
			$Z=20$			
$2s^2 2p^4\ {}^3P_2$	−597.440 366	−0.283 435	0.164 755	−0.008 954	0.125 293	−597.442 707
${}^3P_1$	−597.328 018	−0.283 400	0.163 172	−0.008 931	0.125 556	−597.331 620
${}^3P_0$	−597.308 649	−0.282 744	0.163 454	−0.008 995	0.125 526	−597.311 408
${}^1D_2$	−597.025 259	−0.293 144	0.161 220	−0.009 086	0.125 489	−597.040 781
${}^1S_0$	−596.642 389	−0.267 296	0.164 764	−0.009 476	0.125 315	−596.629 082
$2p^6\ {}^1S_0$	−590.666 278	−0.498 793	0.170 554	−0.010 915	0.114 552	−590.890 880
$2s2p^5\ {}^3P_2^o$	−594.582 179	−0.320 326	0.166 486	−0.009 064	0.119 679	−594.625 404
${}^3P_1^o$	−594.488 081	−0.320 288	0.163 482	−0.009 080	0.119 875	−594.534 092
${}^3P_0^o$	−594.433 960	−0.320 088	0.162 899	−0.009 063	0.120 003	−594.480 209
${}^1P_1^o$	−593.459 504	−0.383 958	0.165 373	−0.009 311	0.119 809	−593.567 591
			$Z=30$			
$2s^2 2p^4\ {}^3P_2$	−1428.775 842	−0.297 610	0.611 680	−0.021 373	0.502 292	−1427.980 852
${}^3P_1$	−1427.952 955	−0.295 526	0.600 502	−0.021 250	0.504 167	−1427.165 062
${}^3P_0$	−1428.290 915	−0.288 872	0.621 636	−0.021 862	0.502 388	−1427.477 626
${}^1D_2$	−1427.527 764	−0.304 812	0.587 395	−0.021 276	0.504 008	−1426.762 449
${}^1S_0$	−1426.432 811	−0.281 786	0.586 579	−0.021 496	0.504 932	−1425.644 582
$2p^6\ {}^1S_0$	−1416.254 678	−0.477 711	0.632 397	−0.023 761	0.454 263	−1415.669 490
$2s2p^5\ {}^3P_2^o$	−1423.362 007	−0.326 416	0.616 724	−0.021 490	0.477 514	−1422.615 674
${}^3P_1^o$	−1422.864 295	−0.331 233	0.609 975	−0.021 512	0.478 262	−1422.128 804
${}^3P_0^o$	−1422.418 578	−0.325 536	0.601 741	−0.021 421	0.479 479	−1421.684 314
${}^1P_1^o$	−1421.239 706	−0.386 455	0.605 864	−0.021 582	0.478 675	−1420.563 205
			$Z=42$			
$2s^2 2p^4\ {}^3P_2$	−2922.340 138	−0.304 231	1.791 013	−0.045 187	1.559 323	−2919.339 220
${}^3P_1$	−2918.371 995	−0.300 300	1.747 678	−0.044 564	1.567 306	−2915.401 874
${}^3P_0$	−2921.450 700	−0.290 081	1.837 186	−0.046 866	1.558 758	−2918.391 702
${}^1D_2$	−2917.803 309	−0.308 348	1.701 775	−0.044 156	1.566 875	−2914.887 163
${}^1S_0$	−2913.501 287	−0.292 188	1.681 969	−0.043 281	1.573 033	−2910.581 754
$2p^6\ {}^1S_0$	−2897.999 767	−0.482 228	1.847 015	−0.050 019	1.400 032	−2895.284 967
$2s2p^5\ {}^3P_2^o$	−2911.388 620	−0.333 063	1.803 053	−0.045 322	1.478 029	−2908.485 923
${}^3P_1^o$	−2910.117 037	−0.357 288	1.807 954	−0.045 848	1.478 532	−2907.233 686
${}^3P_0^o$	−2907.202 211	−0.331 319	1.753 990	−0.044 890	1.486 050	−2904.338 381
${}^1P_1^o$	−2906.050 135	−0.372 589	1.739 755	−0.044 721	1.484 806	−2903.242 884

ing from $2s^2 2p_{1/2}^2 2p_{3/2}^2$ and $2s^2 2p_{3/2}^4$ configurations are nearly degenerate, and there is a strong configuration interaction between them (see Table II). Three-configuration MCDFSCF calculations yield the configuration mixing coefficients, 0.737 246, −0.674 943, and 0.030 330, for the lowest $J=0$ ($^3P_0$) state of Ca^{12+}, yielding coefficients nearly equal in magnitude for the two CSFs arising from the $2s^2 2p_{1/2}^2 2p_{3/2}^2$ and $2s^2 2p_{3/2}^4$. As Z increases, relativity lifts the near degeneracy and significantly weakens the configuration interaction between the two CSFs because it induces a large separation between the $2p_{1/2}$ and $2p_{3/2}$ spinor energies and simultaneously a smaller separation between the $2s_{1/2}$ and $2p_{1/2}$ spinor energies (the $2s_{1/2}$ and $2p_{1/2}$ spinor energies become asymptotically degenerate in the hydrogenic limit).

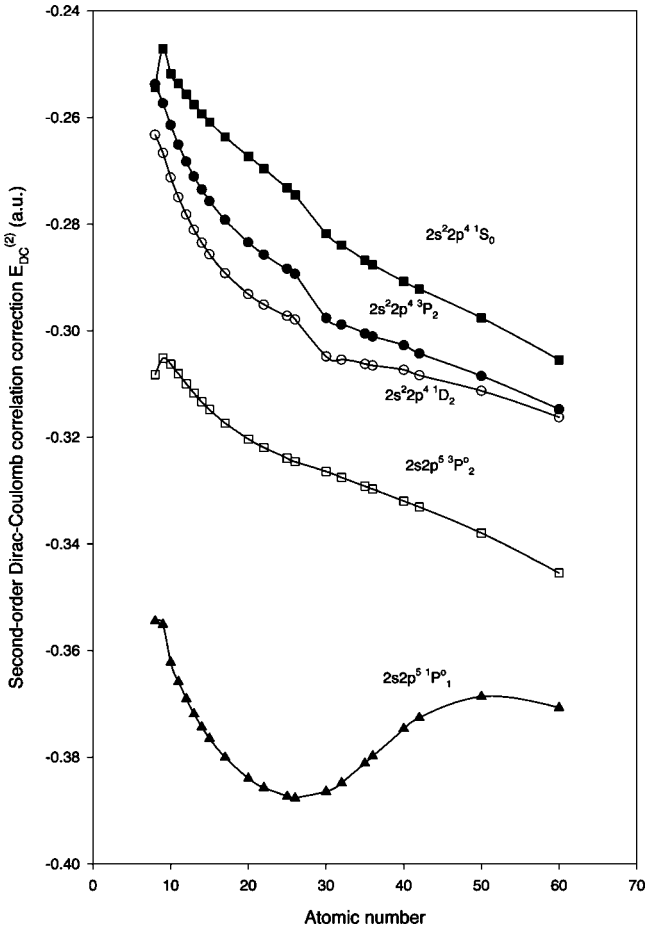

FIG. 1. Second-order Dirac-Coulomb correlation corrections $E_{\mathrm{DC}}^{(2)}$ of five selected states as functions of nuclear charge Z.

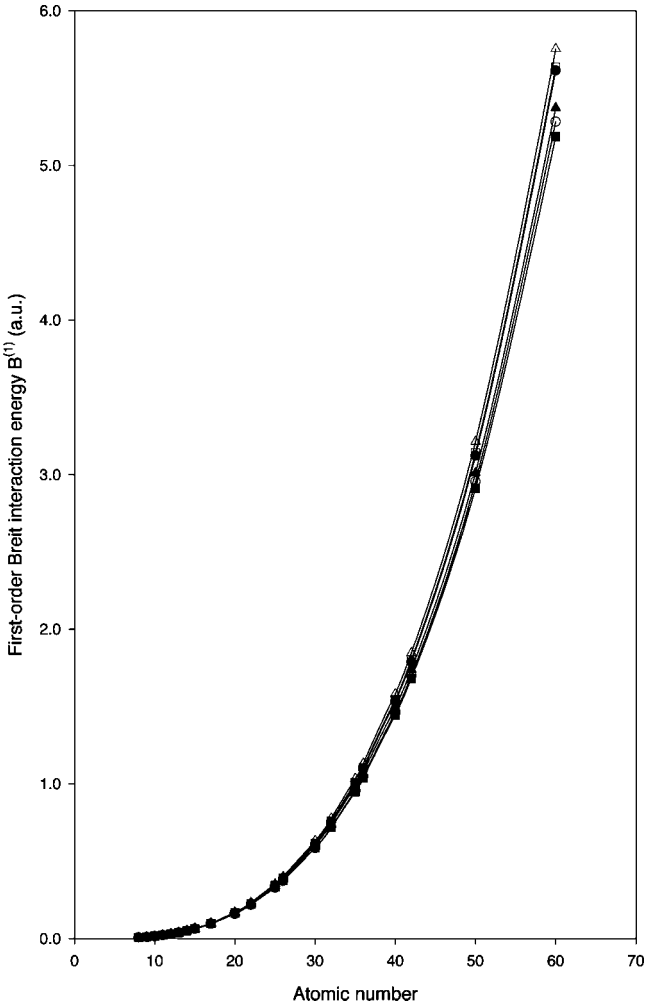

FIG. 2. First-order Breit interaction energies $B^{(1)}$ of five selected states as functions of nuclear charge. Filled circles, triangles, and squares represent, respectively, $2s^22p^4\ ^3P_2$, $2s2p^5\ ^1P_1$, $2s^22p^4\ ^1S_0$. Open circles, triangles, and squares represent, respectively, $2s^22p^4\ ^1D_2$, $2p^6\ ^1S_0$, and $2s2p^5\ ^3P_2$.

Table II displays just such a trend as the nuclear charge increases. A three-configuration MCDFSCF on the $J=0$ state Zn^{22+} yields the configuration mixing coefficients, 0.945 76 and $-0.316\,66$, respectively, for the two CSFs arising from the $2s^22p_{1/2}^2 2p_{3/2}^2$ and $2s^22p_{3/2}^4$. The configuration interaction between the two CSFs for Zn^{22+} ($Z=30$) is reduced dramatically by relativity making $2s^22p_{1/2}^2 2p_{3/2}^2$ the dominant configuration. On the other hand, the $n=2$ complex gives rise to only one CSF for the $J=1$, even-parity state, which comes from the electronic configuration $2s^22p_{1/2}^1 2p_{3/2}^3$. Thus, the $J=1$ state does not exhibit near degeneracy.

Within the $n=2$ complex, the electronic configurations, $2s^22p_{1/2}^2 2p_{3/2}^2$ and $2s^22p_{1/2}^1 2p_{3/2}^3$, give rise to two $J=2$, even-parity CSFs ($^3P_2$ and $^1D_2$), and these interact strongly. Two-configuration MCDFSCF calculations on the ground $^3P_2$ state, including the two $J=2$ CSFs of Ca^{12+}, yield configuration mixing coefficients of 0.903 95 and 0.427 63, indicating near degeneracy, while the configuration mixing coefficients become 0.976 91 and 0.213 64 for the heavier Zn^{22+} with the configuration $2s^22p_{1/2}^2 2p_{3/2}^2$ being more dominant. Again, as Z increases, relativity causes a large separation of the $2p_{1/2}$ and $2p_{3/2}$ spinor energies and weakens the configuration interaction between the $2s^22p_{1/2}^2 2p_{3/2}^2$ and $2s^22p_{1/2}^1 2p_{3/2}^3$ CSF.

In the fourth column of Table I, we present the correlation energies, $E_{\mathrm{corr}}^{\mathrm{MC}}$, recovered from MCDFSCF for the lowest $J=2$ ($^3P_2$) and $J=0$ ($^3P_0$) even-parity states of Ca^{12+} and Zn^{22+} computed in increasing CSF expansion lengths. The correlation energies were computed by subtracting the single configuration DFSCF energies from the MCDFSCF energies [8]. Because of near degeneracy and strong configuration interaction of CSFs, the $J=0$ ($^3P_0$) state yields the largest correlation energy in each MC expansion. At $N_{\mathrm{CSF}}=3$, the $J=0$ ($^3P_0$) state yields correlation energies ($E_{\mathrm{corr}}^{\mathrm{MC}}$) of $-0.396\,712$ a.u. and $-0.308\,182$ a.u., respectively, for Ca^{12+} and Zn^{22+}, the bulk of which are nondynamic correlation energies. The nondynamic correlation becomes noticeably smaller in magnitude in Zn^{22+} than in Ca^{12+} because relativity tends to lift near degeneracy in the $J=0$ state as Z increases.

The bulk of the experimentally determined fine-structure term energies are reproduced by the MCDFSCF calculations within the $n=2$ complex for both Ca^{12+} and Zn^{22+}. In Ca^{12+}, the lowest $J=0$ ($^3P_0$) and $J=1$ ($^3P_1$) state energies computed in the three-configuration MCDFSCF and one-configuration DFSCF calculations are, respectively, 0.131 717 a.u. and 0.112 348 a.u. above the ground $J=2$ ($^3P_2$) state computed in a two-configuration MCDFSCF

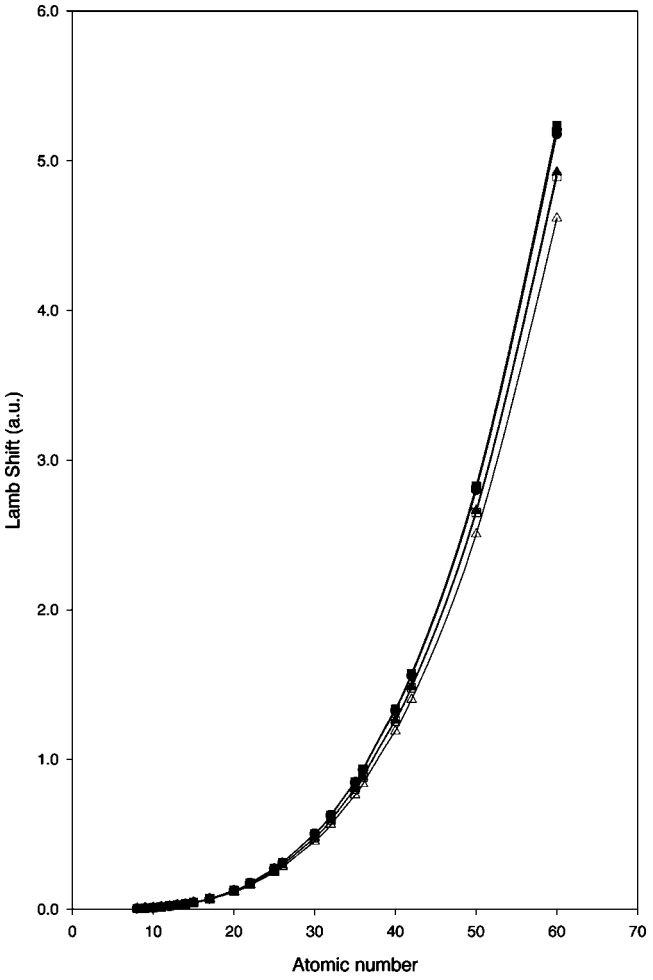

FIG. 3. LSs as functions of nuclear charge. Filled circles, triangles, and squares represent, respectively, $2s^2 2p^4\ ^3P_2$, $2s2p^5\ ^1P_1$, and $2s^2 2p^4\ ^1S_0$. Open circles, triangles, and squares represent, respectively, $2s^2 2p^4\ ^1D_2$, $2p^6\ ^1S_0$, and $2s2p^5\ ^3P_2$.

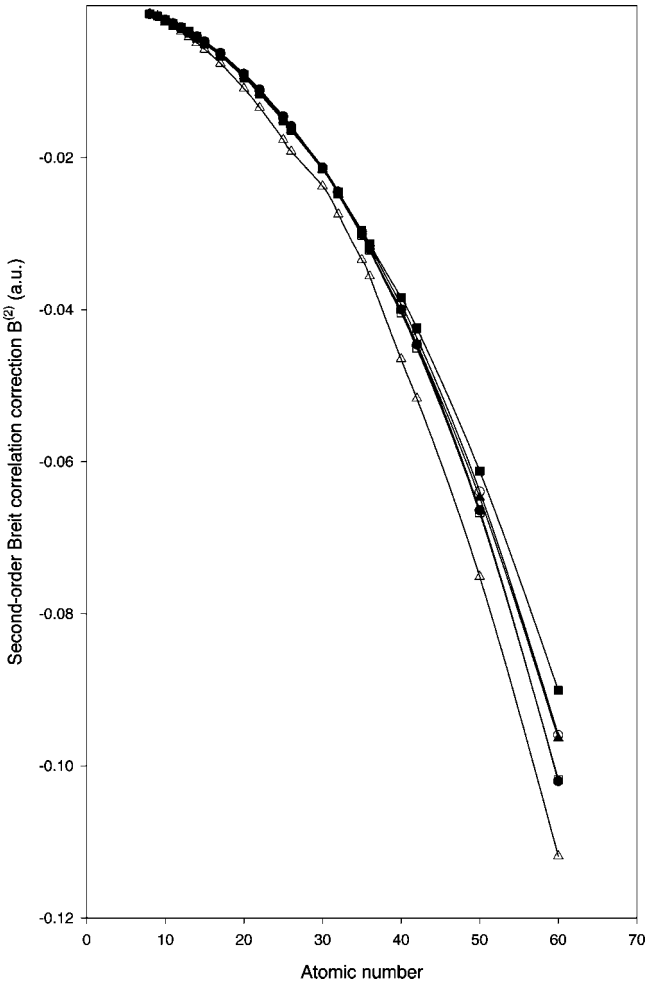

FIG. 4. Second-order Breit correlation corrections $B^{(2)}$ as functions of nuclear charge. Filled circles, triangles, and squares represent, respectively, $2s^2 2p^4\ ^3P_2$, $2s2p^5\ ^1P_1$, and $2s^2 2p^4\ ^1S_0$. Open circles, triangles, and squares represent, respectively, $2s^2 2p^4\ ^1D_2$, $2p^6\ ^1S_0$, and $2s2p^5\ ^3P_2$.

while experimental values are, respectively, 0.131 59 a.u. and 0.11 147 a.u. [37,38]. For Zn^{22+}, the lowest $J=0$ ($^3P_0$) and $J=1$ ($^3P_1$) state energies computed in a three-configuration MCDFSCF and one-configuration DFSCF calculations are, respectively, 0.484 927 a.u. and 0.822 887 a.u. above the ground $J=2$ ($^3P_2$) state computed by a two-configuration MCDFSCF while the corresponding experimental values are, respectively, 0.503 188 a.u. and 0.815 461 a.u. [37,38]. The residual discrepancy is primarily due to dynamic correlation unaccounted for in the MCDFSCF calculations.

To accurately account for dynamic correlation, state-by-state second-order MRMP calculations were performed for each of the three fine-structure states with increasing CSF expansion lengths. All electrons were included in the correlation calculations. Computed second-order DC correlation corrections are given in the fifth column of Table I. The total DC correlation energies, $E_{\rm corr}^{\rm MC}+E_{\rm DC}^{(2)}$, are given in the last column of the table. Because of near degeneracy and strong configuration mixing of CSFs, the $J=0$ even-parity state yields the largest total DC correlation energy. At $N_{\rm CSF}=3$, the $J=0$ ($^3P_0$) states of Ca^{12+} and Zn^{22+} yield total DC correlation corrections of $-0.679\,456$ a.u. and $-0.597\,054$ a.u., respectively. In contrast, single-reference ($N_{\rm CSF}=1$) second-order MP calculations for the $J=0$ ($^3P_0$) states of Ca^{12+} and Zn^{22+} yield total correlation energies of only $-0.396\,032$ a.u. and $-0.442\,840$ a.u., respectively. These account for only 58% and 74%, respectively, of the total DC correlation energies of Ca^{12+} ($=-0.679\,456$ a.u.) and Zn^{22+} ($=-0.597\,054$ a.u.) obtained by a second-order MRMP based on three-configuration MCDF reference wave functions. Failure to treat nondynamic correlation in zero order causes difficulty in recovering a large fraction of dynamic correlation energy. As we have stated earlier, the bulk of the experimentally determined fine-structure separations among the lowest three ($^3P_2$, $^3P_0$, and $^3P_1$) states, are reproduced by the MCDFSCF calculations, which properly treat state-specific nondynamic correlation due to interacting configurations. Once the nondynamic correlation is accounted for by the MCDFSCF, the dynamic DC correlation energies $E_{\rm DC}^{(2)}$ computed by MR-MP are similar in magnitude for all three fine-structure states, i.e., $E_{\rm DC}^{(2)}\approx -0.28$ a.u. and ≈ -0.29 a.u., respectively, for Ca^{12+} and Zn^{22+}.

MCDFSCF and MRMP calculations were carried out on the ground state and nine low-lying excited states of oxygen and 20 oxygenlike ions with $Z=9$, 10, 11, 12, 13, 14, 15, 17,

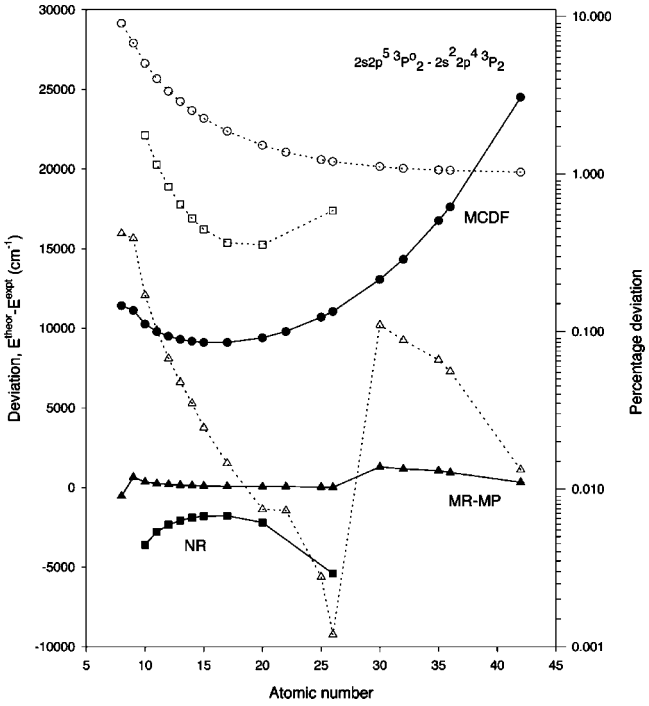

FIG. 5. Deviations from the experiment of the computed term energy separations for the $2s2p^5\ ^3P_2^o - 2s^22p^4\ ^3P_2$ as a function of nuclear charge Z. Deviation (cm^{-1}) and percentage deviation are given, respectively, on the left and right ordinates. Atomic numbers are given on the abscissa. Filled circles, triangles, and squares represent, respectively, deviations of the MCDF, MRMP, and nonrelativistic many-body perturbation-theoretical levels. Open circles, triangles, and squares represent, respectively, percentage deviations of the MCDF, MRMP, and nonrelativistic many-body perturbation-theory calculations.

20, 22, 25, 26, 30, 32, 35, 36, 40, 42, 50, and 60. These ten lowest states consist of two $J=2$ ($^3P_2$ and $^1D_2$) and two $J=0$ ($^3P_0$ and $^1S_0$) even-parity states arising from $2s^22p^4$ configuration, one $J=0$ ($^1S_0$) even-parity state arising from the $2p^6$, and one $J=2$ ($^3P_2^o$), two $J=1$ ($^3P_1^o$ and $^1P_1^o$), and one $J=0$ ($^3P_0^o$) odd-parity states arising from the $2s2p^5$. Two different MC DF SCF methods, J-averaged and state-specific, were employed to obtain the basis spinors for MRMP calculations. J-averaged MCDFSCF calculations were employed for oxygen and oxygenlike ions with $Z=9-26$, and a state-specific MCDFSCF for $Z=30-60$. Critically evaluated experimental data are available for these ions up to $Z=42$ [37,38]. In Table III, we illustrate our calculations on seven representative ions with $Z=10$, 15, 20, 25, 30, 35, and 42. The table displays the MCDFSCF energies, E_{SCF}, MRMP second-order Dirac-Coulomb correlation energies, $E_{\mathrm{DC}}^{(2)}$, first- and second-order Breit interaction energies, $B^{(1)}$ and $B^{(2)}$, radiative corrections, and total energies of the ten lowest states. The radiative corrections, or the electron self-energy and vacuum polarization, estimated by employing the method described in Refs. [33] and [35], are given in the sixth column of the table under the heading ''LS'' (LS for Lamb shift). Figures 1–4 show variations of the computed $E_{\mathrm{DC}}^{(2)}$, $B^{(1)}$, $B^{(2)}$, and LS of several representative states as functions of the atomic number Z. The MC DF energies of the excited $^1D_2$ and $^1S_0$ even-parity states are those obtained in the $^3P_{J=0,2}$ state MC energy optimization; state-by-state MCDFSCF calculations for the excited states were not done. Thus spinors and configuration-mixing coefficients employed in MRMP calculations for the excited states were those obtained in the $^3P_{J=0,2}$ MCDF calculations. Note again that the configuration mixing coefficients displayed in Table II for the ground and excited even-parity states of Ca^{12+} and Zn^{22+} are representative of those obtained in the $^3P_{J=0,1,2}$ MCDF calculations. For $Z=8-26$ and $Z=30-60$, respectively, J-averaged and state-by-state MCDFSCF calculations were performed for the excited $J=0,1,2$ ($^3P_{0,1,2}^o$) odd-parity states. The numbers of reference CSFs for the MCDFSCF and MRMP calculations were, respectively, 3, 1, and 2 for the $J=0$, 1, and 2 even-parity states. For the odd-parity $J=0,1,2$ states, they were, respectively, 1, 2, and 1; these account for all the CSFs arising from the $n=2$ complex. All electrons were correlated in the MRMP calculations. MCDFSCF calculations including the frequency-independent Breit interaction in the configuration-mixing step of the MCSCF algorithm have also been performed to study the effect of the Breit interaction on fine-structure term energies. Energy shifts due to the first-order Breit interactions $B^{(1)}$ thus obtained are given in the fourth column of Table III. The relativistic many-body shifts $B^{(2)}$ [5,6,8] that arise from including the Breit interaction in the effective electron-electron interaction in the second-order MRMP perturbation calculations are also displayed in the fifth column of the table. $B^{(2)}$ is computed as the difference between the second-order correlation correction evaluated with B_{12} [Eq. (4)] in the effective electron-electron interaction and the second-order DC correlation correction, $E_{\mathrm{DC}}^{(2)}$.

Table IV displays the contribution from each order of perturbation theory to energy separation (a.u.) of nine low-lying excited states relative to the ground $2s^22p^4\ ^3P_2$ state of Zn^{22+}. These contributions were computed by subtracting the energy of the ground $2s^22p^4\ ^3P_2$ even-parity state from that of the excited state in each order of perturbation theory displayed in Table III. The last column of Table IV contains the term energy splittings obtained in this study along with those obtained in previous correlated calculations by Cheng, Froese Fischer, and Kim [39] and by experiment for comparison. The MCDFSCF and MRMP calculations, which include the Breit interaction in the effective electron-electron interaction, as well as the Lamb shifts, result in significant corrections and yield close agreement between the calculated and experimental term energy separations, while DC correlation corrections $\Delta E_{\mathrm{DC}}^{(2)}$ alone do not. For the lowest $^3P_0$, $^3P_1$, $^1D_2$, and $^1S_0$ states, the first-order correction $\Delta B^{(1)}$ is much larger than $\Delta E_{\mathrm{DC}}^{(2)}$. The $B^{(1)}$ for the ground and excited states are displayed in Fig. 2 as functions of the atomic number Z. The Lamb shift correction, ΔLS, is comparable or even larger for most states than the relativistic many-body shift $\Delta B^{(2)}$. Because radiative corrections are significantly smaller in higher excited states, ΔLS becomes negative and increases by an order of magnitude for these states. Figure 3 shows the importance of ΔLS in accurately predicting term energy separations. Radiative corrections are noticeably different from state to state. The difference, ΔLS, becomes as large as a few tenths of an a.u. in large-Z ions and results in significant correction to term energy separations, as does $\Delta B^{(1)}$.

TABLE IV. Contribution from each order of perturbation theory to energy separation (a.u.) of nine low-lying excited states relative to the ground $2s^2 2p^4\ ^3P_2$ state of Zn^{22+}. The term energy separations are compared with previous work and with the experiment.

	ΔE_{SCF}	$\Delta E_{\mathrm{DC}}^{(2)}$	$\Delta B^{(1)}$	$\Delta B^{(2)}$	ΔLS[a]	$\Delta E_{\mathrm{total}}$
			$2s^2 2p^4\ ^3P_0$			
MRMP	0.484 927	0.008 738	0.009 956	−0.000 489	0.000 096	0.503 226
Z-expansion[b]	0.484 389	0.0	0.010 174		0.000 096	0.4947
Experiment[c]						0.503188
			$2s^2 2p^4\ ^3P_1$			
MRMP	0.822 887	0.002 084	−0.011 178	0.000 123	0.001 875	0.815 790
Z-expansion[b]	0.822 883	0.0	−0.011 213		0.001 875	0.8135
Experiment[c]						0.815 461
			$2s^2 2p^4\ ^1D_2$			
MRMP	1.248 078	−0.007 202	−0.024 285	0.000 097	0.001 716	1.218 403
Z-expansion[b]	1.247 716	−0.0107	−0.024 427		0.001 716	1.2250
Experiment[c]						1.218 022
			$2s^2 2p^4\ ^1S_0$			
MRMP	2.343 031	0.015 824	−0.025 101	−0.000 123	0.002 640	2.336 270
Z-expansion[b]	2.340 612	0.0248	−0.025 010		0.002 640	2.3430
Experiment[c]						2.335 380
			$2s2p^5\ ^3P_2^o$			
MRMP	5.413 835	−0.028 806	0.005 044	−0.000 117	−0.024 778	5.365 178
Z-expansion[b]	5.413 855	−0.0298	0.005 035		−0.024 778	5.3643
Experiment[c]						5.359 280
			$2s2p^5\ ^3P_1^o$			
MRMP	5.911 547	−0.033 623	−0.001 705	−0.000 139	−0.024 030	5.852 048
Z-expansion[b]	5.911 589	−0.0298	−0.001 649		−0.024 030	5.8561
Experiment[c]						5.845 582
			$2s2p^5\ ^3P_0^o$			
MRMP	6.357 264	−0.027 926	−0.009 939	−0.000 048	−0.022 813	6.296 538
Z-expansion[b]	6.357 317	−0.0298	−0.009 946		−0.022 813	6.2948
Experiment[c]						6.290 367
			$2s2p^5\ ^1P_1^o$			
MRMP	7.536 136	−0.088 845	−0.005 816	−0.000 209	−0.023 617	7.417 647
MR-MP(opt)[d]	7.533 364	−0.086 134	−0.005 735	−0.001 136	−0.023 864	7.416 495
Z-expansion[b]	7.531 790	−0.0924	−0.006 456		−0.023 864	7.4091
Experiment[c]						7.409 740
			$2p^6\ ^1S_0$			
MRMP	12.521 164	−0.180 101	0.020 717	−0.002 388	−0.048 029	12.311 362
MR-MP(opt)[d]	12.498 537	−0.157 495	0.016 288	−0.001 876	−0.048 812	12.306 642
Z-expansion[b]	12.498 391	−0.1604	0.015 956		−0.048 812	12.3051
Experiment[c]						12.290 107

[a]ΔLS is from this work.
[b]Cheng, Froese Fischer, and Kim [39], Z-expansion calculations.
[c]Edlen, [37], Experimental data, Ref. [38].
[d]Optimized spinors from state-specific MC DF.

Cheng, Froese Fischer, and Kim [39] computed the energies of the ground and excited states of oxygenlike ions by the finite-difference MCDFSCF within the $n=2$ complex and estimated the leading nonrelativistic dynamic correlation corrections using the Z-expansion theory of Layzer [21]. Inclusion of the nonrelativistic correlation correction along with the first-order Breit interaction and the Lamb shifts significantly improved agreement between theory and experiment. The term energy separations computed by our MRMP method are in better agreement with the experiment than those obtained by Cheng, Froese Fischer, and Kim [39] for the lowest four excited states. Referring to the last two entries in Table IV, the MR-MP term energy separations deviate from experiment by as much as 0.008 a.u. and 0.0213 a.u., respectively, for the $2s2p^5\ ^1P_1^o$ and $2p^6\ ^1S_0$ states whereas those computed by Cheng, Froese Fischer, and Kim [39] are in better agreement with the experiment. The results suggest that use of the spinors and configuration-mixing coefficients from ground-state MCDFSCF calculations in MRMP calculations for the excited states are less appropriate for higher excited states. State-specific MCDFSCF and MRMP calculations were performed on the excited $2s2p^5\ ^1P_1^o$ and $2p^6\ ^1S_0$ states to examine if the optimum spinors for the excited states improve the term energy sepa-

TABLE V. Energies (cm^{-1}) of low-lying even-parity states of oxygen and oxygenlike ions relative to the ground $2s^2 2p^4\ ^3P_2$ state. The term energy separations, E^{theor}, computed by MRMP are compared with the experiment.

Z	$2s^2 2p^4\ ^3P_1$		$2s^2 2p^4\ ^3P_0$		$2s^2 2p^4\ ^1D_2$		$2s^2 2p^4\ ^1S_0$		$2p^6\ ^1S_0$	
	E^{theor}	E^{expt}	E^{theor}	E^{expt}	E^{theor}	E^{expt}	E^{theor}	E^{expt}	E^{theor}	E^{expt}
60	4338 200		358 573		4479 456		8948 972		14 291 249	
50	1906 359		272 808		2033 780		4039 624		8232 842	
42	864 147	862 684	207 956	214 010	977 113	975 974	1922 041	1924 137	5279 298	5266 180
40	690 130		191 215		799 796		1567 153		4724 041	
36	424 185	423 933	160 088	162 011	525 210	525 066	1020 232	1020 595	3784 241	3777 648
35	371 858	371 663	152 035	153 478	470 804	470 699	912 282	912 501	3579 486	3573 416
32	243 652	243 568	127 401	127 793	336 308	336 229	647 012	646 933	3026 366	3021 332
30	179 045	178 973	110 445	110 437	267 408	267 325	512 752	512 557	2702 031	2697 367
26	89 251	89 439	75 218	75 188	168 792	168 848	324 949	325 149	2132 810	2134 090
25	73 622	73 800	66 524	66 505	150 806	150 851	291 748	291 899	2006 359	2007 816
22	39 180	39 277	42 290	42 309	108 731	108 717	215 516	215 509	1654 291	1656 253
20	24 380	24 465	28 816	28 880	88 212	88 202	178 570	178 568	1437 959	1440 313
17	10 785	10 847	14 056	14 127	64 796	64 782	135 152	135 206	1133 381	1136 464
15	5701	5748	7763	7817	52 266	52 256	110 696	110 799	939 739	943 504
14	3989	4028	5524	5568	46 571	46 568	99 215	99 343	844 854	849 058
13	2702	2733	3791	3827	41 140	41 147	88 052	88 206	750 880	755 634
12	1758	1783	2491	2521	35 901	35 925	77 097	77 287	657 503	662 973
11	1086	1107	1549	1576	30 793	30 841	66 249	66 496	564 276	570 823
10	628	643	899	921	25 759	25 841	55 382	55 751	469 969	478 827
9	331	341	475	490	20 736	20 873	44 593	44 918	399 337	
8	150	158	216	227	15 574	15 868	32 722	33 793	310 737	

TABLE VI. Energies (cm^{-1}) of low-lying odd-parity states of oxygen and oxygenlike ions relative to the ground $2s^2 2p^4\ ^3P_2$ state. The term energy separations, E^{theor}, computed by MRMP are compared with the experiment.

Z	$2s2p^5\ ^3P^o_2$		$2s2p^5\ ^3P^o_1$		$2s2p^5\ ^3P^o_0$		$2s2p^5\ ^1P^o_1$	
	E^{theor}	E^{expt}	E^{theor}	E^{expt}	E^{theor}	E^{expt}	E^{theor}	E^{expt}
60	6760 441		7261 260		11 170 598		11 440 327	
50	3802 980		4181 481		5767 222		6015 455	
42	2382 023	2381 708	2656 857	2650 483	3292 303	3291 573	3532 737	3529 552
40	2117 877		2365 097		2851 851		3092 405	
36	1676 282	1675 351	1866 459	1864 603	2136 839	2135 798	2380 149	2377 764
35	1580 945	1579 903	1756 684	1755 028	1987 396	1986 274	2231 636	2229 358
32	1325 473	1324 308	1458 828	1457 440	1598 310	1597 034	1844 637	1842 732
30	1177 520	1176 226	1284 376	1282 957	1381 930	1380 576	1627 985	1626 251
26	922 855	922 845	984 791	984 692	1029 992	1029 966	1267 771	1267 573
25	866 836	866 813	919 624	919 516	956 445	956 409	1190 112	1189 924
22	712 320	712 268	742 960	742 838	762 079	762 020	978 198	978 007
20	618 326	618 280	638 367	638 266	650 193	650 149	850 489	850 299
17	486 964	486 894	496 384	496 276	501 614	501 554	672 888	672 630
15	403 882	403 784	409 018	408 890	411 787	411 701	560 834	560 476
14	363 286	363 160	366 927	366 774	368 866	368 752	506 096	505 643
13	323 159	323 005	325 653	325 476	326 966	326 824	451 972	451 383
12	283 403	283 212	285 044	284 831	285 898	285 715	398 303	397 485
11	243 929	243 682	244 955	244 688	245 482	245 238	344 928	343 688
10	204 635	204 288	205 236	204 872	205 539	205 195	291 659	289 480
9	165 438	164 798	165 761	165 107	165 918	165 279	238 393	239 605
8	125 731	126 267	125 879	126 340	125 948	126 384	184 216	

rations. The results are given in the second row, denoted by MRMP(opt), in each of the last two entries. Use of the optimum spinors does not significantly improve the computed term energy separation, $2s2p^5\ ^1P_1^o - 2s^22p^4\ ^3P_2$, while the computed separation, $2p^6\ ^1S_0 - 2s^22p^4\ ^3P_2$, improves appreciably and becomes comparable in accuracy with that obtained by Cheng, Froese Fischer, and Kim.

In Tables V and VI, a detailed comparison of theoretical and experimental data is made on the term energies of the low-lying even- and odd-parity states of oxygen and oxygen-like ions with $Z=9-60$, given relative to the ground $2s^22p^4\ ^3P_2$ state. Theoretical term energy separations, E^{theor}, of the low-lying excited states were computed by subtracting the total energy of the ground $2s^22p^4\ ^3P_2$ state from those of the excited levels. Experimental term energy separations E^{expt} [37,38] are reproduced in an adjacent column for comparison. Experimental data are not available for ions with $Z=40$, 50, and 60.

Figure 5 illustrates the differences and percentage deviations, $100|E^{\text{theor}}-E^{\text{expt}}|/E^{\text{expt}}$, between theoretical and experimental term energy separations, $2s2p^5\ ^3P_2^o - 2s^22p^4\ ^3P_2$, as functions of the atomic number Z. We see that the theoretical term energy separations differ from the experiment by amounts ranging from $10\,\text{cm}^{-1}$ at $Z=26$ to $1294\,\text{cm}^{-1}$ at $Z=30$ in the range $8\leqslant Z\leqslant 42$. Although the percentage deviation between theory and experiment increases to the level of a few tenths of a percent near the low-Z end, it is consistently below 0.1% in the range $10\leqslant Z\leqslant 42$, quite good agreement. The differences between the term energy separations computed by the nonrelativistic many-body perturbation theory [40] and those obtained by the experiment are also given for comparison. In the nonrelativistic calculations, the multireference second-order perturbation theory was employed to account for electron correlation for the ions with $10\leqslant Z\leqslant 26$. Relativistic corrections were included in the Breit-Pauli approximation. The term energy separations computed by relativistic MRMP differ from experiment by 0.1% or less for intermediate Z up to $Z=42$, except at the low-Z end where the discrepancy increases up to 0.4%. Nonrelativistic many-body perturbation calculations deviate by 3% from the experiment at $Z=10$. The percentage deviation reduces monotonically in the range $11\leqslant Z\leqslant 20$ and increases again as Z approaches 26, again due to the inadequacy of the Breit-Pauli approximation. The accuracy of the nonrelativistic and relativistic calculations for the low-Z ions is limited by the approximate treatment of electron correlation. The deviations between theory and experiment computed solely at the MCDFSCF level (filled circles in Fig. 5) are large throughout Fig. 5. However, subsequent inclusions of dynamic correlation by MRMP and of radiative corrections significantly reduce the deviation.

V. CONCLUSIONS

We have developed a relativistic multireference Møller-Plesset perturbation theory for a general class of openshell systems with a manifold of configurations, which interact strongly due to asymptotic degeneracy. The multireference perturbation theory for electron correlation is designed to treat a general class of openshell systems with two or more valence electrons that often exhibit quasidegeneracies. The essential features of the theory are its treatment of the state-specific nondynamic correlation in zero order through a MC DFSCF, and recovery of the remaining correlation, which is predominantly dynamic pair correlation, by second-order perturbation theory. We have reported the first successful implementation and application of relativistic multireference Møller-Plesset perturbation theory based on MCDFSCF reference functions to ions of oxygen isoelectronic sequences. Accurate calculation of term energy separations in such systems requires a method flexible enough to account for static correlation (near degeneracy), which varies considerably from state to state.

ACKNOWLEDGMENT

The authors thank Dr. Y.-K. Kim at the National Institute of Standards and Technology for providing us with a code to evaluate radiative corrections described in Refs. [33] and [35].

[1] J. P. Desclaux, At. Data Nucl. Data Tables **12**, 311 (1973); Comput. Phys. Commun. **9**, 31 (1975); in *Atomic Theory Workshop on Relativistic and QED Effects in Heavy Atoms*, Gaithersburg, MD, 1985, edited by H. P. Kelly and Y-K. Kim, AIP Conf. Proc. No. 136 (AIP, New York, 1985), p. 162.

[2] I. P. Grant, B. J. McKenzie, P. H. Norrington, D. F. Mayers, and N. C. Pyper, Comput. Phys. Commun. **21**, 207 (1980); F. A. Parpia, C. Froese Fischer, and I. P. Grant, *ibid.* **94**, 249 (1996).

[3] K. T. Cheng, Y.-K. Kim, and J. P. Desclaux, At. Data Nucl. Data Tables **24**, 111 (1979).

[4] M. H. Chen, in *X-Ray and Atomic Inner-Shell Physics*, edited by B. Crasemann (AIP, New York, 1982) p. 331; M. H. Chen and B. Crasemann, Phys. Rev. A **28**, 2829 (1983); **30**, 170 (1984).

[5] W. R. Johnson and J. Sapirstein, Phys. Rev. Lett. **57**, 1126 (1986); W. R. Johnson, S. A. Blundell, and J. Sapirstein, Phys. Rev. A **37**, 307 (1988); **42**, 1087 (1990).

[6] S. A. Blundell W. R. Johnson, and J. Sapirstein, Phys. Rev. Lett. **65**, 1411 (1991); S. A. Blundell, J. Sapirstein, and W. R. Johnson, Phys. Rev. D **45**, 1602 (1992).

[7] H. M. Quiney, I. P. Grant, and S. Wilson, Phys. Scr. **36**, 460 (1987); H. M. Quiney, I. P. Grant, and S. Wilson, in *Many-Body Methods in Quantum Chemistry, Lecture Notes in Chemistry* edited by U. Kaldor (Springer, Berlin, 1989); H. M. Quiney, I. P. Grant, and S. Wilson, J. Phys. B **23**, L271 (1990).

[8] Y. Ishikawa, Phys. Rev. A **42**, 1142 (1990); Y. Ishikawa and H. M. Quiney, *ibid.* **47**, 1732 (1993); Y. Ishikawa and K. Koc, *ibid.* **50**, 4733 (1994).

[9] Y. Ishikawa and K. Koc, Phys. Rev. A **53**, 3966 (1996); **56**, 1295 (1997).

[10] K. Koc and J. Migdalek, J. Phys. B **23**, L5 (1990); **25**, 907 (1992).

[11] A. W. Weiss and Y.-K. Kim, Phys. Rev. A **51**, 4487 (1995).

[12] Z. W. Liu and H. P. Kelly, Phys. Rev. A **43**, 3305 (1991).
[13] E. Avgoustoglou, W. R. Johnson, D. R. Plante, J. Sapirstein, S. Sheinerman, and S. A. Blundell, Phys. Rev. A **46**, 5478 (1992); E. Avgoustoglou, W. R. Johnson, Z. W. Liu, and J. Sapirstein, *ibid.* **51**, 1196 (1995); M. S. Safronova, W. R. Johnson, and U. I. Safronova, *ibid.* **53**, 4036 (1997).
[14] E. N. Avgoustoglou and D. R. Beck, Phys. Rev. A **57**, 4286 (1998).
[15] V. A. Dzuba, V. V. Flambaum, and M. G. Kozlov, Phys. Rev. A **54**, 3948 (1996); V. A. Dzuba and W. R. Johnson, *ibid.* **57**, 2459 (1998).
[16] D. R. Beck, Phys. Rev. A **37**, 1847 (1988); D. R. Beck and Z. Cai, *ibid.* **37**, 4481 (1988); Z. Cai and D. R. Beck, *ibid.* **40**, 1657 (1989); D. R. Beck and D. Datta, *ibid.* **44**, 758 (1991); D. R. Beck, *ibid.* **45**, 1399 (1992); **56**, 2428 (1997); K. D. Dinov and D. R. Beck, *ibid.* **53**, 4031 (1996).
[17] J. C. Morrison and C. Fischer, Phys. Rev. A **35**, 2429 (1987); S. Salomonson, I. Lindgren, and A.-M. Mårtensson, Phys. Scr. **21**, 351 (1980); E. Lindroth and A.-M. Mårtensson-Pendrill, Phys. Rev. A **53**, 3151 (1996).
[18] K. Hirao, Chem. Phys. Lett. **190**, 374 (1992); **201**, 59 (1993); H. Nakano, J. Chem. Phys. **99**, 7983 (1993).
[19] H.-J. Werner, Adv. Chem. Phys. **69**, 1 (1987); H.-J. Werner and W. Meyer, J. Chem. Phys. **73**, 2342 (1980).
[20] K. Wolinski, H. L. Sellers, and P. Pulay, Chem. Phys. Lett. **140**, 225 (1987); R. B. Murphy and R. P. Messmer, *ibid.* **183**, 493 (1991); K. Andersson, P. Malmqvist, and B. O. Roos, J. Phys. Chem. **96**, 1218 (1992); P. Kozlowski and E. R. Davidson, J. Chem. Phys. **100**, 3672 (1994); K. G. Dyall, *ibid.* **102**, 4909 (1995).
[21] D. Layzer, Ann. Phys. (N.Y.) **8**, 271 (1959); D. Layzer and J. Bahcall, *ibid.* **17**, 177 (1962).
[22] M. J. Vilkas, Y. Ishikawa, and K. Koc, Phys. Rev. E **58**, 5096 (1998); Chem. Phys. Lett. **280**, 167 (1997).
[23] I. P. Grant, in *Relativistic, Quantum Electrodynamic, and Weak Interaction Effects in Atoms*, Proceedings of the Conference on Relativistic, Quantum Electrodynamic, and Weak Interaction Effects in Atoms, Santa Barbara, CA, 1988, edited by W. R. Johnson, P. Mohr, and J. Sucher, AIP Conf. Proc. No. 189 (AIP, New York, 1989), p. 209.
[24] J. Sucher, Phys. Rev. A **22**, 348 (1980).
[25] M. H. Mittleman, Phys. Rev. A **24**, 1167 (1981).
[26] Y. Ishikawa, H. M. Quiney, and G. L. Malli, Phys. Rev. A **43**, 3270 (1991); K. Koc and Y. Ishikawa, *ibid.* **49**, 794 (1994); Y. Ishikawa, K. Koc, and W. H. E. Schwarz, Chem. Phys. **225**, 239 (1997).
[27] C. Møller and M. S. Plesset, Phys. Rev. **46**, 618 (1934).
[28] P. J. Mohr, Phys. Rev. A **46**, 4421 (1992); P. J. Mohr and Y.-K. Kim, *ibid.* **45**, 2727 (1992); P. J. Mohr, G. Plunien, and G. Soff, Phys. Rep. **293**, 227 (1998).
[29] S. A. Blundell, P. J. Mohr, W. R. Johnson, and J. Sapirstein, Phys. Rev. A **48**, 2615 (1993).
[30] J. Sapirstein, Phys. Scr. **36**, 801 (1987); Nucl. Instrum. Methods Phys. Res. B **31**, 70 (1988); S. Mallampalli and J. Sapirstein, Phys. Rev. A **54**, 2714 (1996); **57**, 1548 (1998).
[31] L. Labzowsky, V. Karasiev, I. Lindgren, H. Persson, and S. Salomonson, Phys. Scr. **T46**, 150 (1993); I. Lindgren, H. Persson, S. Salomonson, V. Karasiev, L. Labzowsky, A. Mitrushenkov, and M. Tokman, J. Phys. B **26**, L503 (1993); I. Lindgren, H. Persson, S. Salomonson, and L. Labzowsky, Phys. Rev. A **51**, 1167 (1995).
[32] G. W. F. Drake, Adv. At. Mol. Phys. **18**, 399 (1982).
[33] P. Indelicato, O. Gorceix, and J. P. Desclaux, J. Phys. B **20**, 651 (1987).
[34] M. W. Schmidt and K. Ruedenberg, J. Chem. Phys. **71**, 3951 (1979).
[35] Y.-K. Kim, in *Atomic Processes in Plasmas*, Gaithersburg, MD, 1989, edited by Y. K. Kim and R. C. E Hon, AIP Conf. Proc. No. 206 (AIP, New York, 1990), p. 19.
[36] T. Kagawa, Phys. Rev. A **22**, 2340 (1980).
[37] B. Edlén, Phys. Scr. **28**, 51 (1983).
[38] J. R. Fuhr, W. C. Martin, A. Musgrove, J. Sugar, and W. L. Wiese, NIST Atomic Spectroscopic Database, available at http://physics.nist.gov/PhysRefData/contents.html.
[39] K. T. Cheng, C. Froese Fischer, and Y.-K. Kim, J. Phys. B **15**, 181 (1982).
[40] G. Gaigalas, J. Kaniauskas, R. Kisielius, G. Merkelis, and M. J. Vilkas, Phys. Scr. **49**, 135 (1994).